THE JOURNAL OF BIOLOGICAL CHEMISTRY VOL. 282, NO. 24, pp. 17877–17889, June 15, 2007

Transcriptional Activators and Repressors for the Neuron-specific Expression of a Metabotropic Glutamate Receptor*[S]

Received for publication, January 5, 2007, and in revised form, April 3, 2007 Published, JBC Papers in Press, April 12, 2007, DOI 10.1074/jbc.M700149200

Luca Crepaldi[‡], Carmen Lackner[‡], Corrado Corti[§], and Francesco Ferraguti[‡1]

From the [‡]Department of Pharmacology, Innsbruck Medical University, Peter-Mayr-Strasse 1a, A-6020 Innsbruck, Austria and the [§]Department of Biology, Psychiatry Centre of Excellence in Drug Discovery, GlaxoSmithKline Medicines Research Centre, 37135 Verona, Italy

Metabotropic glutamate receptor 1 (mGlu1) has a discrete distribution in the central nervous system restricted to neurons. Its expression undergoes important changes during development and in response to physiological and pathological modifications. Here, we have determined the structure of the mGlu1 gene and demonstrated that mGlu1 transcription takes places at alternative first exons. Moreover, we have identified active promoter regions upstream from the two most expressed first exons by means of luciferase reporter gene assays performed in primary cerebellar granule neurons. Targeted mutations of active elements constituting the core promoter and electrophoretic mobility shift assays demonstrated that the factors thyroid transcription factor-1 and CCAAT/enhancer-binding proteins β act synergistically to promote mGlu1 transcription. We have also elucidated the molecular bases for the neuron-specific expression of mGlu1 identifying a neural restrictive silencing element and a regulatory factor for X box element, which suppressed mGlu1 expression in nonneuronal cells. These results reveal the molecular bases for cell- and context-specific expression of an important glutamate receptor critically involved in synaptogenesis, neuronal differentiation, synaptic transmission, and plasticity.

Specific strategies mediating positive gene regulation or repression are required to generate tissue and cell type diversity. Among the tissues composing higher organisms, the central nervous system appears characterized by the highest complexity in terms of specialization and cell subtypes. To understand how the interplay of multiple transcription factors regulates cell-specific expression of neuronal genes, it is critical to define regulatory sequence elements in specific promoters of genes with a well characterized anatomical profile.

Glutamate is the primary excitatory neurotransmitter in the mammalian central nervous system, where it plays a critical role in neuronal differentiation, synaptic transmission, and plasticity through the activation of ionotropic and metabotropic (mGlu)[2] receptors (1). The significance of genetic control over glutamatergic transmission is underscored by the temporal and cell-specific expression of its receptors in the developing and mature brain.

In the last decade, many efforts have been directed at analyzing the promoter(s) of glutamate receptor genes (2–7), yet for most of them a precise identification of the *cis*-regulatory elements and cognate transcription factors mediating tissue-specific and stimulus/context-dependent expression is still missing.

To date, eight mGlu subtypes have been cloned and divided into three groups according to their sequence homology, intracellular coupling, and pharmacological properties (8). The mGlu1 gene (*Grm1*) shows a discrete distribution in the brain, including the cerebellum, hippocampus, and olfactory bulbs, predominantly restricted to neurons (9). Four alternatively spliced isoforms of mGlu1 have been identified (10–12), each displaying area- and cell-specific expression (13–15). Several physiological and pathological conditions are characterized by important changes in both mGlu1 mRNA and protein levels. A progressive increase of mGlu1 expression occurs during development (16), and Cajal-Retzius cells, which regulate neuronal migration during cortical development, were shown to display mGlu1α expression from E18 to P10 (17). The importance of regulating mGlu1 is also emphasized by the observation that mice lacking this receptor develop a severe motor impairment, have altered synaptic plasticity (18), and maintain a multiple innervation of cerebellar Purkinje cells by climbing fibers (19). Moreover, ectopic expression of mGlu1 in both mouse and human melanocytes has been implicated in melanoma-genesis and metastasis (20).

Chromosomal mapping of *Grm1* was achieved in rats (1p13) and humans (6q24) (21, 22), whereas in mice it was mapped to chromosome 10 band a1 by transcript mapping (available on the World Wide Web at www.ncbi.nlm.nih.gov/unigene).

* This work was supported by Austrian Science Foundation Fonds zur Förderung der wissenschaftlischen Forschung Grant P16720 (to F. F.). The costs of publication of this article were defrayed in part by the payment of page charges. This article must therefore be hereby marked "*advertisement*" in accordance with 18 U.S.C. Section 1734 solely to indicate this fact.

[S] The on-line version of this article (available at http://www.jbc.org) contains supplemental Tables 1 and 2 and Figs. 1 and 2.

[1] To whom correspondence should be addressed. Tel.: 43-512-9003-71204; Fax: 43-512-9003-72300; E-mail: francesco.ferraguti@i-med.ac.at.

[2] The abbreviations used are: mGlu, Metabotropic glutamate receptor; C/EBP, CCAAT/enhancer-binding protein; NRSF, neural restrictive silencing factor; RFX, regulatory factor for X box; RACE, rapid amplification(s) of cDNA ends; TIS, transcription initiation site; BHK, baby hamster kidney; TSA, trichostatin A; CGC, cerebellar granule cell; ANOVA, analysis of variance; EMSA, electrophoretic mobility shift assay; ChIP, chromatin immunoprecipitation; NRSE, neural restrictive silencer element; RT, reverse transcriptase; ECR, evolutionary conserved region; TTF, thyroid transcription factor; HDAC, histone deacetylase.

TABLE 1
Constructs used in luciferase reporter gene assays

Construct	Sequence (relative to first TIS)	Source	Vector
−2097/ExIa	−2097/+108:1501/+1819	PAC library, CRB cDNA	pGL3-basic
−1108/ExIa	−1108/+108:1501/+1819	PAC library, CRB cDNA	pGL3-basic
−599/ExIa	−599/+108:1501/+1819	Restriction enzyme digestion (OliI)	pGL3-basic
−123/ExIa	−123/+108:1501/+1819	Restriction enzyme digestion (BstEII)	pGL3-basic
−68/ExIa	−68/+108:1501/+1819	Deletion by PCR	pGL3-basic
−11/ExIa	−11/+108:1501/+1819	Restriction enzyme digestion (SpeI)	pGL3-basic
−1108/−123:−11/ExIa	−1108/−123:−11/+108:1501/+1819	Restriction enzyme digestion (BsteII/SpeI)	pGL3-basic
+895/ExII	+895/+1819	PAC library	pGL3-basic
+1088/ExII	+1088/+1819	PAC library	pGL3-basic
−1108/*Grm1*	−1108/+1819	PAC library	pGL3-basic
+478/+899/SV40	+478/+899	*Grm1*(−1108)	pGL3-promoter

However, neither the 5′-structure nor the transcriptional activators and repressors of *Grm1* have yet been uncovered.

In this work, we have determined the structure of *Grm1* and demonstrated that its transcription is initiated at different alternative first exons. Moreover, we have identified both positive and negative regulatory sequence elements responsible for neuron-specific expression of mGlu1. We established a synergistic role of the transcription factors thyroid transcription factor (TTF)-1 and CCAAT/enhancer-binding protein β (C/EBPβ) to promote mGlu1 transcription. On the other hand, the neural restrictive silencing factor (NRSF)/RE-1-silencing transcription factor and the regulatory factor for X box (RFX) produced transcriptional inactivation of *Grm1* in nonneuronal cells. These results reveal the molecular bases for cell- and context-specific expression of mGlu1 and may provide a key to understand the mechanism(s) responsible for altered regulation of mGlu1 expression in pathological conditions, such as in melanocytic neoplasia (20).

EXPERIMENTAL PROCEDURES

5′-Rapid Amplification of cDNA Ends (RACE)—The transcription initiation sites (TISs) of the human and mouse mGlu1 gene were determined by 5′-RACE using whole mouse brain and human hippocampal and cerebellar Marathon-Ready cDNA (Clontech). Two rounds of PCR were performed for each of the 5′-RACE. Sequences and annealing temperatures of primers are shown in supplemental Table 1. Oligonucleotides were purchased from Microsynth GmbH (Balgach, Switzerland). Taq polymerase was purchased from Promega. PCR products were subcloned into the pCR2.1-TOPO vector (Invitrogen) and sequenced by a dye terminator cycle sequencing reaction (Microsynth).

RNA Extraction, RNase Protection Assay, and Reverse Transcription (RT)-PCR—Total RNA from different adult male mouse (C57Bl/6) brain areas or from NIH-3T3 cells was extracted using Trizol (Invitrogen), according to the product specifications.

RNase protection assays were performed using the RPA III kit (Ambion), as previously described (6). Probe exon Ia encompassed exons Ia and II (bp +1/+108 and +1501/+1656, where +1 corresponds to the most 5′ TIS in exon Ia). Probe II encompassed exon II (bp +1266/+1656). A probe encoding for actin was used as control. RNA Century Marker Plus Template Set (Ambion) was used to generate a radiolabeled molecular weight ladder.

First strand cDNAs were obtained by reverse transcription, performed on 5 μg of total RNA according to Superscript II reverse transcriptase (Invitrogen) specifications, primed either with random hexamers or with a gene-specific primer (m*GRM1*_rev_05). Oligonucleotide primers (Microsynth GmbH) used for the detection of mGlu1 alternative first exons, mGlu1α and -β isoforms, and β-actin are listed in supplemental Table 1.

Reporter Gene Constructs and Mutagenesis—Reporter gene constructs were prepared by subcloning of DNA fragments obtained from restriction enzyme digestion and/or PCR amplification of PAC clones or, when necessary (*e.g.* to obtain exonic DNA sequences), of a cerebellar cDNA library. The mouse genomic DNA PAC library RPCI21, spotted on nylon membranes (Human Genome Mapping Project Resource Centre, UK), was screened by hybridization with a radiolabeled probe (Highprime kit (Roche Applied Science) and Redivue [α-^{32}P]dCTP (Amersham Biosciences), ~3000 Ci/mmol), corresponding to the KpnI-SacII restriction fragment of the rat mGlu1 cDNA sequence (accession M61099) sharing 99% identity with the homologous mouse sequence. The identified clones were confirmed by means of PCR (supplemental Table 1). Constructs used in reporter gene assays are listed in Table 1. Oligonucleotide primers used for the generation of the constructs are listed in supplemental Table 1. Promoter regions were subcloned into KpnI/XhoI sites of the reporter vectors pGL3-basic or pGL3-promoter (Promega). Constructs used for the deletion scan analysis were obtained by mutating short intervals of 15–20 bp to an EcoRI restriction site in the construct ExIa(−123). Constructs −1108/ExIa/TATAm, −1108/ExIa/INIm, −1108/ExIa/T-Im, −1108/*Grm1*/NRSEm, and +895/exII/RFXm were generated introducing specific mutations by means of the QuikChange II site-directed mutagenesis kit (Stratagene). All constructs were sequenced by a dye terminator cycle sequencing reaction (Microsynth).

Cell Cultures and Transfections—Baby hamster kidney fibroblasts (BHK) were cultured in Dulbecco's modified Eagle's medium/Ham's F-12 medium plus Iscove's modified Eagle's medium (1:1) (PAA Laboratories), supplemented with 10% fetal calf serum, 2 mM glutamine, 100 units/ml penicillin, and 100 μg/ml streptomycin (Invitrogen), maintained at 37 °C in a humidified 5% CO_2 atmosphere. NIH-3T3 fibroblasts were cultured in Dulbecco's modified Eagle's medium (Sigma) supplemented with 10% fetal calf serum, 2 mM glutamine, 100 units/ml penicillin, and 100 μg/ml streptomycin (Invitrogen),

maintained at 37 °C in a humidified 10% CO_2 atmosphere. In selected experiments, cells were treated with trichostatin A (TSA) (Sigma).

Reporter gene constructs were transfected into BHK fibroblasts by means of JetPEI (Qbiogene). Two days after transfection, cells were processed for a luciferase assay. To normalize for the transfection efficiency, a plasmid encoding the *Renilla reniformis* luciferase was co-transfected in a 1:50 ratio. Either pRL-SV40, encoding for the SV40 promoter, or pRL-TK, encoding for the thymidine kinase promoter, was used (Promega). pRL-TK plasmid was used to analyze the neural restrictive silencer element (NRSE), since we repeatedly observed that co-transfection of pRL-SV40 with constructs encoding NRSE always resulted in a ~80% reduction of *Renilla* luciferase activity. Conversely, constructs carrying a specific mutation of NRSE did not have any effect on pRL-SV40 activity. The induction of *Renilla* luciferase by pRL-TK was unaffected.

Primary cerebellar granule cells (CGCs) were obtained from P8 mouse pups as previously described (23). Briefly, cerebella were dissected and minced in Krebs-Ringer buffer and subsequently treated with 50 μg/ml trypsin, 1 mM EDTA for 20 min at 37 °C. Cells were recovered in complete medium (basal medium Eagle's supplemented with 10% fetal calf serum, 10% horse serum, 2 mM glutamine, 0.1% glucose, 25 mM KCl, 100 units/ml penicillin, 100 μg/ml streptomycin) and resuspended at 10^8 cells/ml before electroporation (EasyjecT Plus electroporator; Equibio). Cells were electroporated (2-mm cuvette, 1250 V/cm, 25 microfarads, 99 ohms, 2.47 ms) with 3 μg of DNA and incubated for 10 min at room temperature. The pRL-SV40 plasmid was co-transfected in a 1:20 ratio. Cells were plated into 35-mm Petri dishes at a density of $3 \times 10^5/cm^2$. After 24 h, 10 μM 1-(β-D-arabinofuranosyl)-cytosine (Sigma) was added. Two days after seeding, cells were processed for the luciferase assay.

Luciferase Assays—Firefly and *Renilla* luciferase expression levels were quantified by means of the Dual-Glo luciferase assay system (Promega), according to the manufacturer's specifications. Light emission was measured using a 5-s time frame with a Centro LB 960 luminometer (Berthold Technologies). Results are presented as mean ± S.E. Statistical analysis was performed by one-way ANOVA followed by Bonferroni's *post hoc* test. The confidence limits at the 5% level were considered statistically significant.

Immunofluorescence—Immunoreactivity for mGlu1α was analyzed in CGCs after 6 days in culture by immunofluorescence. Electroporation transfection rate was assessed by transfecting CGCs with pEGFP-N2 plasmid (Clontech). Cells were washed with phosphate-buffered saline, fixed 30 min at room temperature with a ~0.2% picric acid, 4% paraformaldehyde solution made in 0.1 M phosphate buffer. After extensive washes with Tris-buffered saline, cells were incubated for 1 h in blocking solution (20% horse serum, 0.1% Triton X-100 in Tris-buffered saline) and then overnight at 4 °C with primary antibodies (rabbit polyclonal anti-mGlu1α (1:500; Diasorin) and rabbit polyclonal anti-GFP antibody (1:1000; Molecular Probes, Inc., Eugene, OR) made up in 1% horse serum, 0.1% Triton X-100 in Tris-buffered saline. Immunoreactivity was visualized using donkey anti-rabbit secondary antibodies (1:1000) conjugated to the fluorochrome Alexa 488 (Molecular Probes). Cell nuclei were stained by incubating with 2 μg/ml 4′,6-diamidino-2-phenylindole.

TABLE 2
Oligonucleotides used for electrophoretic mobility shift assays

Double-stranded DNA oligonucleotide	Sequence (5′–3′)
Probe E1	TTTCCCTTGCGGTATAATAG
Probe E2	ATAGTGTTGAAGAAAGAGGG
Probe E1m	TTTTCCCGAATTCTAATAGT
Probe E2m	AATAGTGGAATTCAGAGGGC
C/EBPcons	TGCAGATTGCGCAATCTGCA
TTF-1	CTGCCCAGTCAAGTGTTCTT
Steroidogenic factor-1	AAGGCTCAAGGTCACAGACA
RFX-*Grm1*	CAGGCGTTGCCTTAGTAACTAATAT
RFX-MAP1A	CGGCGTTGCCATGGAGACAACTGGC

Electrophoretic Mobility Shift Assay (EMSA)—In order to extract nuclear proteins, BHK cells were rinsed with cold phosphate-buffered saline containing 1 mM sodium orthovanadate, harvested, and resuspended in buffer A (10 mM Hepes, pH 7.9, 10 mM KCl, 1.5 mM $MgCl_2$, 0.5 mM EDTA, 0.5 mM EGTA, 0.6% Igepal CA630) supplemented with protease and phosphatase inhibitors (1 μg/ml aprotinin, leupeptin, chymostatin, antipain, bacitracin, pepstatin A, 10 μg/ml bestatin, 0.5 mM phenylmethylsulfonyl fluoride, 1 mM sodium orthovanadate, 50 mM NaF, 5 mM sodium pyrophosphate). After 5 min on ice, cells were centrifuged for 10 min at 800 × *g*, at 4 °C. The pellets, containing the cell nuclei, were then resuspended in buffer C (20 mM Hepes, pH 7.9, 420 mM KCl, 1.5 mM $MgCl_2$, 0.5 mM EDTA, 10% glycerol) with inhibitors and incubated 30 min on ice. After a centrifugation at 11,000 × *g* for 15 min at 4 °C, the supernatant was collected and frozen in liquid nitrogen. C57Bl/6 mouse cerebella were homogenized in a potter (Potter S; Sartorius) in buffer A without Igepal CA630. After five homogenization strokes, Igepal CA630 was added to a final concentration of 0.5%, followed by five additional strokes. Homogenates were incubated for 10 min and centrifuged at 11,000 × *g* for 1 min at 4 °C. Pelleted nuclei were resuspended in buffer C and incubated for 15 min on ice. After a further centrifugation step, the supernatant was collected and frozen in liquid nitrogen.

Specific probes for EMSA were purchased as single-stranded oligonucleotides (Microsynth GmbH; listed in Table 2). After annealing, 5 pmol of double-stranded DNA oligonucleotide were labeled with [γ-^{32}P]ATP (800 Ci/mmol; Amersham Biosciences) using T4-PNK (Promega) and purified by means of Sephadex G-25 Quick Spin columns (Roche Applied Science).

Nuclear extracts (2–10 μg) were preincubated 15 min at room temperature (30 min in supershift experiments) in binding buffer (10 mM HEPES, pH 7.9, 50 mM KCl, 5 mM $MgCl_2$, 0.2 mM EDTA, 0.1 mM EGTA, 1 mM dithiothreitol, 5% glycerol) with 0.5–1 μg of poly(dI-dC) (Amersham Biosciences) in a final volume of 15 μl. In competition experiments, an exceeding amount (40 pmol) of unlabeled double-stranded DNA oligonucleotides was used. In supershift experiments, 5 μg of specific antibodies (C/EBPα 14AA, C/EBPβ C-19, and C/EBPδ C-22; Santa Cruz Biotechnology) were added. Subsequently, 5×10^5 cpm of radiolabeled probe were added and incubated 15 min at room temperature. DNA-protein complexes were resolved onto a 5% polyacrylamide gel for at least 1.5 h, allowing the unshifted probe to be eluted from the gel. The gel was dried and exposed for autoradiography using Eastman Kodak Co. BioMax MR films.

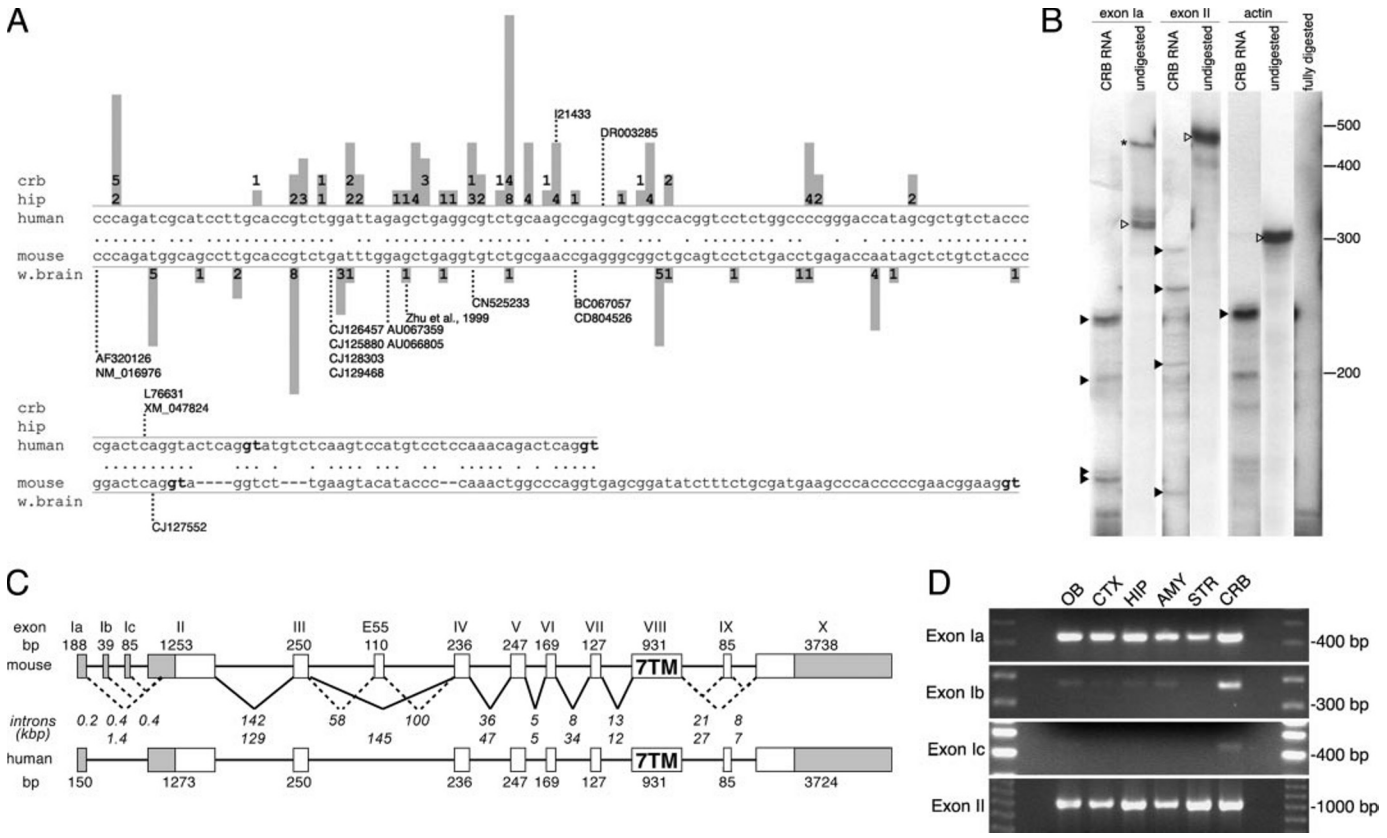

FIGURE 1. **Characterization of *Grm1* TISs, genomic structure, and analysis of alternative first exon expression.** *A*, annealed sequences of human and mouse *Grm1* exon Ia, as obtained by 5′-RACE and public sequence data bases. The *digits* associated with nucleotides indicate the number of 5′-RACE clones starting at that position. The *height* of *histograms* is proportional to the number of clones. The start positions of known cDNAs or expressed sequence tags are indicated by their accession number or reference. Splice donors are indicated in *boldface type*. *B*, RNase protection assay. Multiple protected bands are generated by probes encoding exon Ia and II, whereas a single band is generated by the control β-actin probe (*filled arrowheads*, *lanes 1*, *3*, and *5*). Undigested probes are shown (*open arrowheads*). A high molecular weight self-annealing product (*asterisk*, *lane 2*) was produced by the undigested exon Ia probe, which however did not produce nonspecific bands due to self-protection (*lane 7*). *C*, complete genomic structure of mouse and human *Grm1*, based on 5′-RACE data and public genomic, cDNA, and expressed sequence tag sequences. Alignments were performed by BLAST 2.0. Protein coding regions and 5′- or 3′-untranslated regions are indicated by *open* and *gray boxes*, respectively. Constitutive and alternative splicing are indicated by *filled* and *dashed lines*, respectively. The size of exons is given in bp and in kbp (in *italic type*) for introns. *D*, regional distribution of *Grm1* transcripts generated from alternative first exons. The experiments shown are representative of at least four replicates. *OB*, olfactory bulb; *CTX*, cortex; *HIP*, hippocampus; *AMY*, amygdala; *STR*, striatum; *CRB*, cerebellum.

Chromatin Immunoprecipitation (ChIP) Assay—Chromatin immunoprecipitation was performed using the Upstate ChIP assay kit and anti-NRSF antibody (catalog number 07-579; Upstate Biotechnology). NIH-3T3 cells were fixed for 10 min at 37 °C in 1% formaldehyde. Cells were then washed twice with phosphate-buffered saline with protease inhibitors (1 mM phenylmethylsulfonyl fluoride, 1 μg of aprotinin, 1 μg/ml pepstatin A), resuspended in lysis buffer (Upstate Biotechnology) with inhibitors, incubated for 10 min on ice, and sonicated with a Branson Sonifier Cell Disruptor B-30. Shearing of DNA in 200–1000-bp fragments was assessed by electrophoresis. For ChIP assays on tissue, C57Bl/6 male mice were perfused transcardially for 10 min with 1% paraformaldehyde made in 0.1 M phosphate buffer. Tissue samples (30 mg) were dissected, washed twice in phosphate-buffered saline with protease inhibitors, and homogenized. Dissociated cells were resuspended in lysis buffer with inhibitors and sonicated as described above. The ChIP procedure was then carried out according to the manufacturer's specifications. Immunoprecipitated genomic DNA was analyzed by PCR (supplemental Table 2).

RESULTS

Genomic Structure of Grm1—The 5′-extent of mGlu1 transcripts was determined by 5′-RACE on mouse whole brain and human cerebellar and hippocampal poly(A)$^+$ RNA. For each reaction, 120 clones were sequenced. The results of the 5′-RACE experiments are summarized in Fig. 1 and in supplemental Fig. 1. In both species, the vast majority of TIS clustered onto two different exons that we named exon Ia and exon II (Fig. 1, *A* and C; supplemental Fig. 1). In exon Ia of both species, two alternative splice donor sites were identified, which were located in mouse *Grm1* at +108 and +188 downstream from the most 5′-TIS (+1); the relative usage of these alternative splice sites was 92 and 8%, respectively. Exon II, which contains the ATG codon for the initiation of translation, extended by 552 bp at its 5′-end from the ATG in mouse, hence 233 bp upstream from the known splice acceptor site. Two additional alternative first exons, represented by two single clones obtained from the mouse whole brain 5′-RACE, were identified and named Ib and Ic (Fig. 1*C*; supplementary Fig. 1).

The existence of multiple transcription initiation sites within exons Ia and II was confirmed by RNase protection assays per-

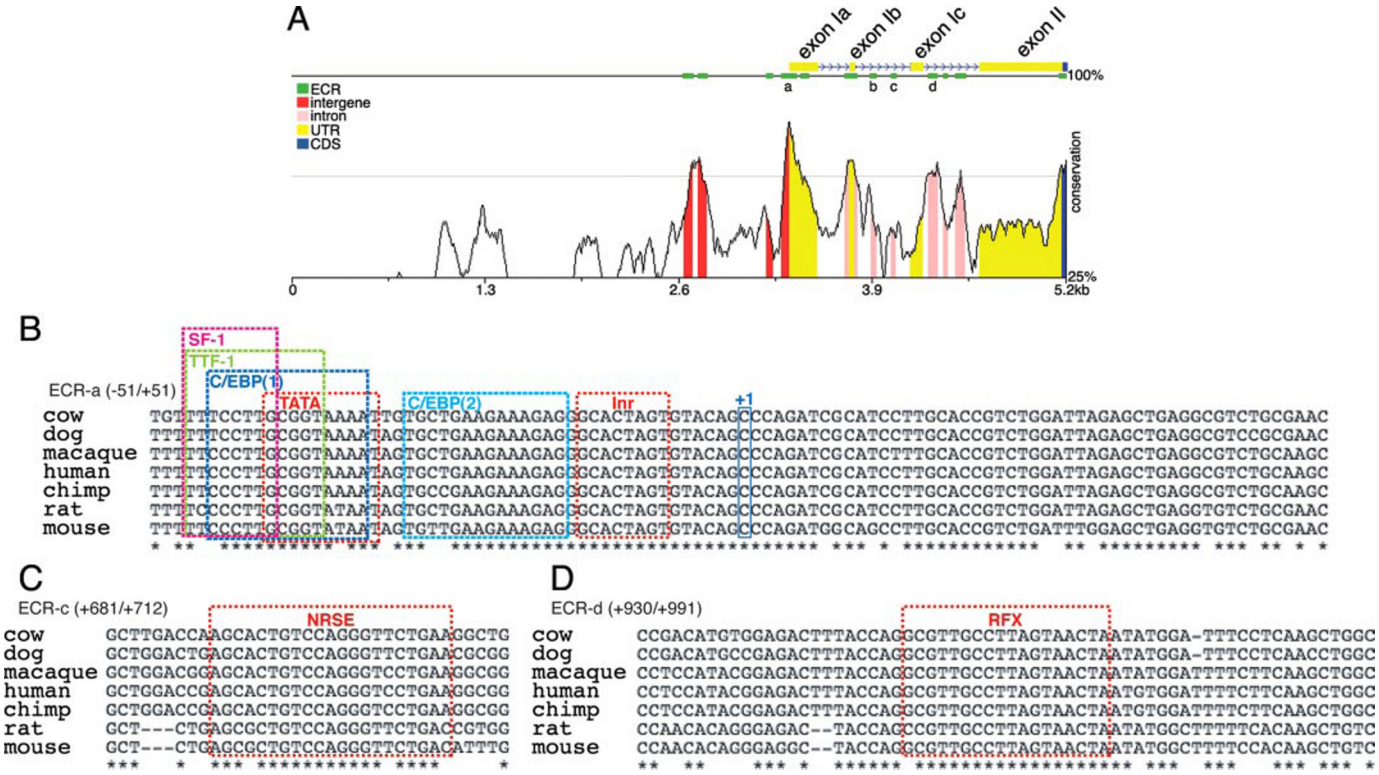

FIGURE 2. ***In silico* analysis of *Grm1* putative promoters.** *A*, phylogenetic shadowing of *Grm1* 5′-region from *Bos taurus*, *C. familiaris*, *Macaca mulatta*, *Homo sapiens*, *Pan troglodytes*, *R. norvegicus*, and *M. musculus* (reference sequence), as obtained by Mulan, setting ECR length at≥30 bp and conservation at ≥70%. ECR-b encompasses a $(GT)_{27}$ repeat. *B*, alignment of ECR-a, containing several putative transcription factor binding sites. *C*, alignment of ECR-c, encoding a putative NRSE. *D*, alignment of ECR-d, encoding a putative RFX element.

formed on total mouse cerebellar RNA (Fig. 1*B*). Two specific cRNA probes were used. The first encompassed the whole exon Ia and part of exon II up to the ATG, joined at the most used splice site; the second probe encoded exon II from its 5′-end up to the ATG. Several RNase-protected fragments were detected by both *Grm1* exon Ia and exon II probes, consistent with the different mRNA forms identified by 5′-RACE (Fig. 1*B*). The undigested probe for exon Ia displayed self-annealing properties, producing a second high molecular weight band (Fig. 1*B*). However, no nonspecific products due to self-protection were detected when the probe was incubated with unrelated yeast tRNA.

We determined the exon/intron arrangement of mouse, human (Fig. 1*C*; supplementary Fig. 2), and rat (not shown) *Grm1* by *in silico* analysis of our 5′-RACE data and public genomic, cDNA, and expressed sequence tag sequences (Fig. 1*C*; supplemental Fig. 2). The human *GRM1* was found to span ~410 kbp and to consist of 10 exons varying from 85 (exon IX) to 3724 bp (exon X) in length (Fig. 1*C*). Intron/exon splice junctions conformed to the GT-AG rule of splice donor/acceptor sites (supplemental Fig. 2). Comparison of *Grm1* in the three species revealed a highly conserved structure in terms of exon/intron organization, size, and sequence identity (supplemental Fig. 2). However, a divergence between human and rodents was the absence in the former of exon E55 (Fig. 1*C*) (12). The insertion between exons III and IV of the alternatively spliced exon E55, which contains an in-frame stop codon, generates a transcript that probably encodes for a truncated protein corresponding to portion of the extracellular domain of mGlu1 (12). The degree of identity between mouse exons Ib and Ic and the corresponding human genomic regions was relatively high (93 and 63%, respectively), but no 5′-RACE clones starting within these exons were found in human samples. The low number of 5′-RACE clones found for these exons suggests a very low and/or highly restricted expression.

We then investigated the regional expression of mGlu1 mRNA isoforms, starting from the different *Grm1* first exons, by RT-PCR analysis (Fig. 1*D*). Expression of transcripts starting within exons Ia and II was detected in all brain areas analyzed, consistent with the 5′-RACE data and confirming a prominent expression of these mRNA forms (Fig. 1*D*). Conversely, exons Ib and Ic were found mainly expressed in cerebellum, whereas they were hardly detectable in other areas (Fig. 1*D*).

A phylogenetic shadowing and multiple alignment on ~5 kb of genomic DNA upstream from the *Grm1* translational start site of seven different mammalian species was performed using the Mulan and MultiPipMaker software (24, 25). Several evolutionary conserved regions (ECRs) were identified, which might encode for transcription-regulatory elements (Fig. 2*A*). The highest level of conservation was found to correspond to putative promoter regions located upstream from first exons.

The identification by 5′-RACE, both in human and mouse, of different mGlu1 mRNAs encoded by alternative first exons, strongly suggested the existence of alternative promoters. *In silico* analysis of *Grm1* putative promoter regions by means of the rVISTA software (26) revealed 249 putative transcription factor binding sites conserved in four species (*Mus musculus*, *Rattus norvegicus*, *Canis familiaris*, and *Homo sapiens*) and dis-

playing relatively high scores (matrix similarity ≥0.80 and core similarity ≥0.95; see supplemental Table 2). Some of these elements were of particular interest for the identification of key *cis*-regulatory elements for mGlu1 transcription. Within the ECR-a, a TATA box and an Initiator element (Fig. 2*B*) were found with optimal interspacing and distance from the TIS (27), hence suggesting that these two elements constitute the *Grm1*-exon Ia core promoter. Additional elements, such as two C/EBPs, the steroidogenic factor-1 and the TTF-1, were also identified and might represent alternative transcriptional modules (Fig. 2*B*). No obvious core promoter elements were found upstream from exon II, even if a putative TATA box (+1048/+1057) was present 218 bp upstream from the first TIS within exon II. Although the typical distance between a TATA box and the TIS ranges between 31 and 26 bp, active TATA boxes were found farther upstream (28). Similarly to exon II, no obvious core promoter elements were identified upstream from exons Ib and Ic.

We found a highly conserved NRSE in the intronic region corresponding to ECR-c, between exons Ib and Ic (positions +687/+707; Fig. 2*C*). NRSE is present in several genes selectively expressed in neurons (29); hence, it could control the specific neuronal expression of mGlu1. A conserved RFX binding site was also identified in the intronic region between exons Ic and II at +951/+968 (Fig. 2*D*). We judged this element of particular interest, since it was recently reported to participate in cell-specific expression of neuronal genes (30, 31).

Finally, a conserved $(GT)_{27}$ simple repeat was found at position +539, between exons Ib and Ic. These repeats are known to influence gene transcription by assuming a Z-DNA conformation, thus altering the DNA looping properties (32).

Functional Analysis of Mouse Grm1 Promoter Activity—We performed luciferase reporter gene assays subcloning the 5′-intronic regions flanking exons Ia and II of mouse *Grm1* into the pGL3-basic vector. To obtain the template for the subcloning, we screened the mouse genomic DNA PAC library RPCI21 and identified four clones (390C5, 475L21, 613N10, and 649K24) containing the 5′ region of *Grm1*. Upon transient transfection, the transcriptional activity of these constructs was tested in primary mouse cerebellar granule cells and in BHK fibroblasts as reference. This neuronal preparation has been largely used as a model to analyze mGlu1 signaling and pharmacological profile (33, 34). Moreover, CGCs have the great advantage over other primary neuronal cultures of being relatively homogeneous, since >80% of the cells are granule neurons. Despite the extensive use of CGCs to investigate biochemical and pharmacological properties of mGlu1, no detailed analysis of the expression of this receptor in these cells has ever been performed. We assessed the localization of mGlu1α in cultured CGCs by immunofluorescence, which revealed a relatively small group of neurons (<1%) intensely stained (Fig. 3*A*), whereas most of the granule cells showed only low to very low perisomatic mGlu1α immunolabeling (Fig. 3*B*). Despite this unexpected finding, it is difficult to correlate expression levels with functional measures, since a very efficient coupling of the receptor with intracellular transduction mechanisms might have compensated for the low expression in previous pharmacological and biochemical studies (33, 34).

Transfection of CGCs was performed by electroporation, which with our optimized conditions gave an 8–12% transfection rate (Fig. 3*C*). The analysis of the promoter region upstream from exon Ia was performed on a set of constructs with serial deletions from position −2097 to −11, in which exon Ia, spliced at the most 5′-splice donor site (+108), was joined to exon II up to the ATG codon (region +1501/+1819). In CGCs, constructs carrying serial 5′-deletions of the region −2097 to −68 displayed a high and similar transcriptional activity ranging from 77.0 ± 25.1% (plasmid −2097/ExIa) to 105.2 ± 8.6% (plasmid −599/ExIa) of pGL3-control luciferase activity (Fig. 3*D*). On the other hand, the construct lacking virtually all of the genomic region upstream from exon Ia (plasmid −11/ExIa) displayed a luciferase activity similar to the promoterless vector pGL3-basic (Fig. 3*D*). Analogous results were obtained in BHK fibroblasts, in which the constructs with deletions from −2097 to −599 displayed similar luciferase induction ranging from 8.3 ± 0.4-fold (plasmid −599/ExIa) to 9.5 ± 0.5-fold (plasmid −1108/ExIa) over pGL3-basic (Fig. 3*D*). Further deletions produced a gradual reduction of the transcriptional activity (Fig. 3*D*), although it remained clearly above pGL3-basic. Likewise in CGCs, plasmid −11/ExIa showed no significant activity in BHK cells (Fig. 3*D*). These results clearly indicated that the minimal region sufficient to drive transcription at the *Grm1* exon Ia promoter resides within a region comprised between −68/−11. In agreement, luciferase activity was abolished completely by the deletion of the region −123/−11 in both CGCs and BHK cells (Fig. 3*D*).

In order to characterize in more detail the core promoter, we performed a deletion scan analysis of the region −123/−8 using plasmid −123/ExIa as a template, in which seven consecutive regions of ~15 bp were mutated to an EcoRI restriction site (Fig. 3*E*). Deletions ΔD (−68/−53) to ΔG (−26-11) reduced luciferase activity almost completely in CGCs (Fig. 3*E*) and caused a significant reduction in BHK cells (Fig. 3*E*), indicating that each of these four regions encodes elements essential for basal transcription.

The analysis of the promoter region upstream from exon II was carried out using a construct encoding the whole exon II sequence and the 372-bp intron between exons Ic and II (plasmid +895/ExII) as well as a second construct carrying a 5′-deletion of 193 bp (plasmid +1088/ExII) (Fig. 3*F*). These plasmids produced little or no induction of luciferase activity (22.3 ± 3.0%) (Fig. 3*F*) when tested in CGCs, although plasmid +895/ExII showed nominal statistical significance. Unlike in CGCs, plasmid +895/ExII showed a clear activity in BHK cells (3.6 ± 0.2-fold over pGL3-basic), and the 5′-deletion resulted in a significant enhancement of its activity (5.1 ± 0.4-fold over pGL3-basic), indicating the presence of a silencing element(s), active in fibroblasts, within the region +895/+1088.

The ability of the region −68/−11 in *Grm1* exon Ia promoter to drive basal transcriptional activity prompted us to perform a more refined functional analysis of the putative transcription factor binding elements identified *in silico* (Fig. 4*A*). Using plasmid −1108/ExIa as template, we mutated the putative TATA box and/or the Initiator element (35, 36) and tested the effect of these mutations in luciferase assays (see Table 3). Surprisingly, neither the single nor the double mutations were effective in

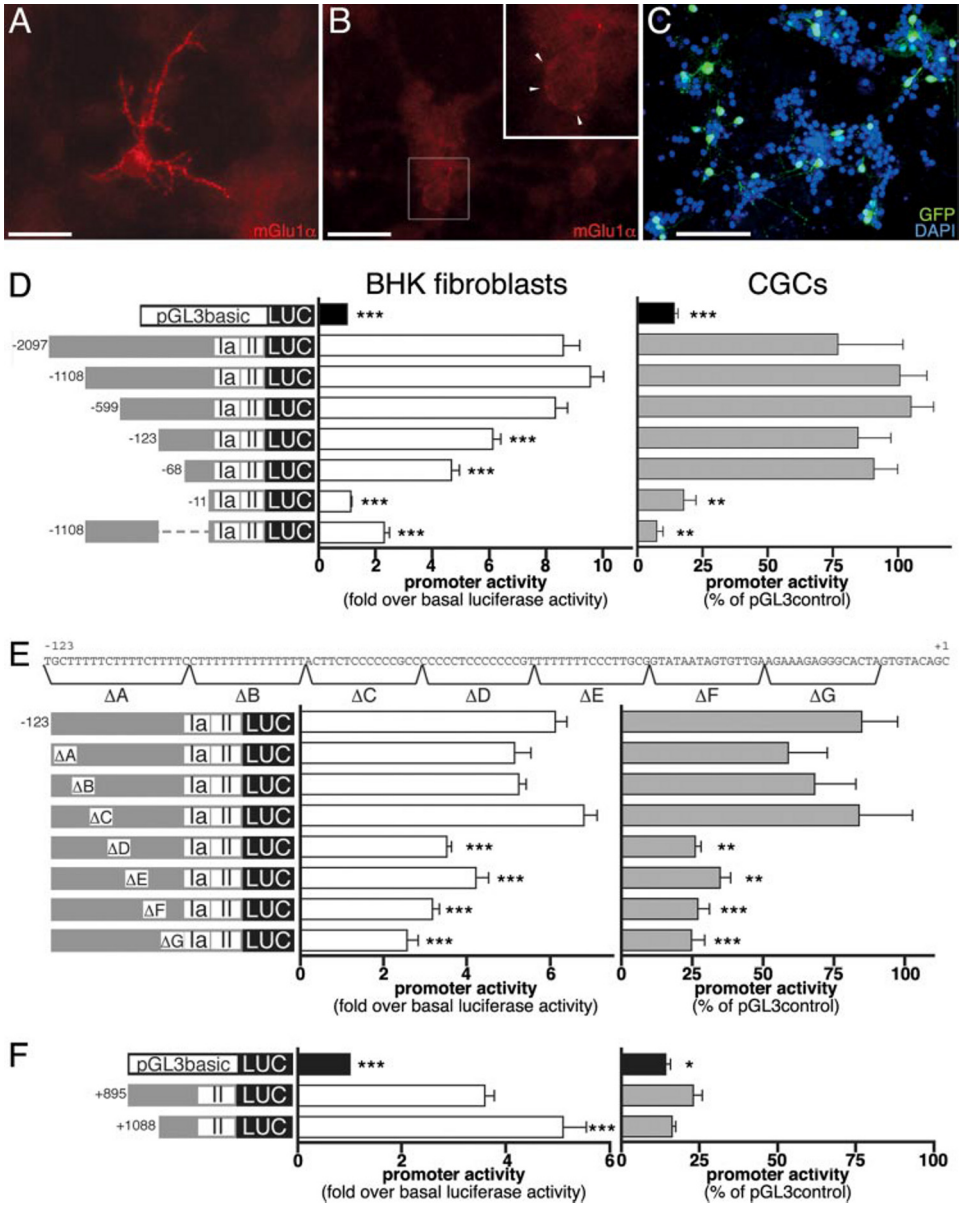

FIGURE 3. **Characterization of CGCs as model for reporter gene assays and analysis of transcriptional activity of *Grm1* promoters.** *A*, immature Purkinje cell or interneuron showing high somatodendritic mGlu1α immunolabeling. *B*, granule cells displaying weak mGlu1α perisomatic labeling. *Scale bar*, 25 μm. A higher magnification of a weakly labeled CGC is shown in the *inset*. The *arrowheads* indicate immunoreactivity associated with the plasma membrane. *C*, EGFP immunofluorescence and 4′,6-diamidino-2-phenylindole counterstaining of electroporated CGCs. The experiments shown are representative of at least three replicates. *Scale bar*, 100 μm. *D–F*, schematic diagrams of reporter gene constructs used in luciferase assays. For BHK cells, activity is given as -fold over pGL3-basic (*white bars*). For CGCs, activity is indicated as a percentage of pGL3-control (*gray bars*); activity of pGL3-basic is indicated by *black bars*. *D*, effect of consecutive deletions of the promoter region upstream from exon Ia. Data are from at least 16 and six replicates for BHK cells and CGCs, respectively. Statistical significance is relative to construct −1108/ExIa. *E*, deletion scan analysis of exon Ia core promoter. The sequence −123/+1 and the deleted regions are shown. Data are from at least eight and four replicates for BHK cells and CGCs, respectively. Statistical significance is relative to construct −123/ExIa. *F*, effect of consecutive deletions of promoter region upstream from exon II. Data are from at least 18 and seven replicates for BHK cells and CGCs, respectively. Statistical significance is relative to construct +895/ExII. *, $p < 0.05$; **, $p < 0.01$; ***, $p < 0.001$, ANOVA with Bonferroni's *post hoc* test.

reducing the transcription driven by exon Ia promoter in both CGCs and BHK fibroblasts (Fig. 4*B*).

On the basis of the putative elements predicted *in silico*, we mutated also two 8-bp-long regions at positions −43/−36 and −27/−20 (indicated as E1 and E2) (Fig. 4*C*) to an EcoRI restriction site using plasmid −123/ExIa as template. Region E1 encompasses the core binding sequences for C/EBP, steroidogenic factor-1 and TTF-1 transcription factors, whereas region E2 encompasses the core binding sequence for a C/EBP (Fig. 4*A*). Moreover, we generated a double mutant construct mutating E1 and E2 to EcoRI and SacI restriction sites, respectively. In CGCs, the mutation of any of the two regions, as well as the double mutation suppressed completely the luciferase activity (Fig. 4*C*), indicating that elements present in E1 and E2 are necessary, but not sufficient to induce transcription. In BHK cells, the single mutations reduced, although not completely, the transcriptional activity of plasmid −123/ExIa (Fig. 4*C*), whereas the double mutation abolished the induction almost completely (Fig. 4*C*). Taken together, these results indicate the presence of a core promoter upstream from *Grm1* exon Ia constituted by two consecutive and synergistic elements.

Electrophoretic Mobility Shift Assays on Grm1 Exon Ia Core Promoter Elements—The actual binding of the predicted transcription factors to the *Grm1* exon Ia core promoter was tested by EMSAs. For this purpose, two double-stranded DNA oligonucleotide probes were designed to encompass the region containing the C/EBP, steroidogenic factor-1, and TTF-1 elements (-49/-30; probe E1) or the C/EBP (-34/-15; probe E2) (Fig. 5*A*). When incubated with nuclear extracts from mouse cerebellum, the radiolabeled probe E1 produced two shifted bands (Fig. 5*B*), which were characterized by competition assays using an exceeding amount of several different unlabeled oligonucleotides. Both bands, as expected, were competed by the cold probe E1. The lower band was specifically competed by a probe for TTF-1, derived from the thyroglobulin gene promoter (37), whereas competition with consensus probes for steroidogenic factor-1 or C/EBP was ineffective. The upper band appeared to derive from nonspecific binding, since it was competed by various probes, such as E1m, which carries the same mutation as construct −123/ExIa/E1m, the consensus probe for C/EBP and a

sequence-unrelated probe specific for RFX binding (Fig. 5*B*). To confirm the binding of TTF-1 to the *Grm1* core promoter region, the consensus sequence for TTF-1 was also used for EMSA. The TTF-1 radiolabeled probe gave rise to a single band when incubated with nuclear extracts from mouse cerebellum (Fig. 5*C*) or CGCs (Fig. 5*D*), which was almost completely displaced by the competition with the unlabeled probe E1. These data, hence, confirmed the specific interaction between TTF-1 and the *Grm1* core promoter.

The radiolabeled probe E2 produced four distinct bands when incubated with nuclear extracts from BHK cells (Fig. 5*E*). Competition assays showed that the upper two bands derive from the interaction with factors of the C/EBP family, since an unlabeled C/EBP consensus probe competed them completely (Fig. 5*E*). Consistent with this finding, probe E2m, which encodes the same mutation as construct −123/ExIa/E2m, was unable to compete any of these two bands. Supershift assays, performed using antibodies specific for the different C/EBP isoforms α, β, and δ, showed that probe E2 is bound by C/EBPβ, at least in BHK extracts (Fig. 5*F*). We failed to detect any significant band shift when probe E2 was incubated with nuclear extracts from cerebellum, although different amounts of nuclear extracts and radiolabeled probe E2 were tested to enhance the sensitivity of the assays. This could depend on many different reasons (*e.g.* low expression levels of C/EBP factors in cerebellum and/or a low affinity of C/EBP to the E2 region).

Identification of an Active NRSE Regulating Grm1 Expression in Nonneuronal Cells—Under physiological conditions, mGlu1 expression is restricted to neuronal cells. Because NRSF has been shown to suppress the expression of neuronal genes in nonneuronal tissues, we investigated the role of the putative NRSE located between *Grm1* exons Ib and Ic in the suppression of mGlu1 expression in fibroblasts. We subcloned a region of ~3 kbp of genomic DNA upstream from the ATG (region −1108/+1819) into pGL3-basic and mutated selectively the NRSE (38) (see Table 3). Luciferase assays performed in BHK cells showed that construct −1108/+1819 induced a very weak, although significant, transcriptional activity (1.2 ± 0.1-fold over pGL3-basic) (Fig. 6*A*). Mutation of the NRSE enhanced the luciferase activity ~3-fold (Fig. 6*A*), demonstrating that this element has a repressive effect on the transcription of *Grm1*. To evaluate more accurately the silencing properties of the NRSE encoded in *Grm1*, we subcloned a 422-bp cassette containing this element (+478/+899) upstream from the SV40 promoter in the pGL3-promoter vector (plasmid +478/+899/SV40). The insertion of this cassette in pGL3-promoter produced a dramatic reduction in luciferase activity, which was largely reverted by the specific mutation of NRSE (plasmid +478/+899/SV40/NRSEm) (Fig. 6*B*). However, mutation of the NRSE was not sufficient to rescue the full transcriptional activity of the SV40 promoter, probably because the insertion of a cassette of this size had an nonspecific negative effect on transcription. These data clearly demonstrate that the NRSE in *Grm1* acts as a strong repressor of transcription in nonneuronal cells and that it can effectively silence a strong promoter, such as SV40.

We further demonstrated the interaction of NRSF with its consensus NRSE located within *Grm1* by chromatin immunoprecipitation. Genomic DNA encompassing this element was immunoprecipitated by means of specific NRSF antibodies from NIH-3T3 fibroblasts and,

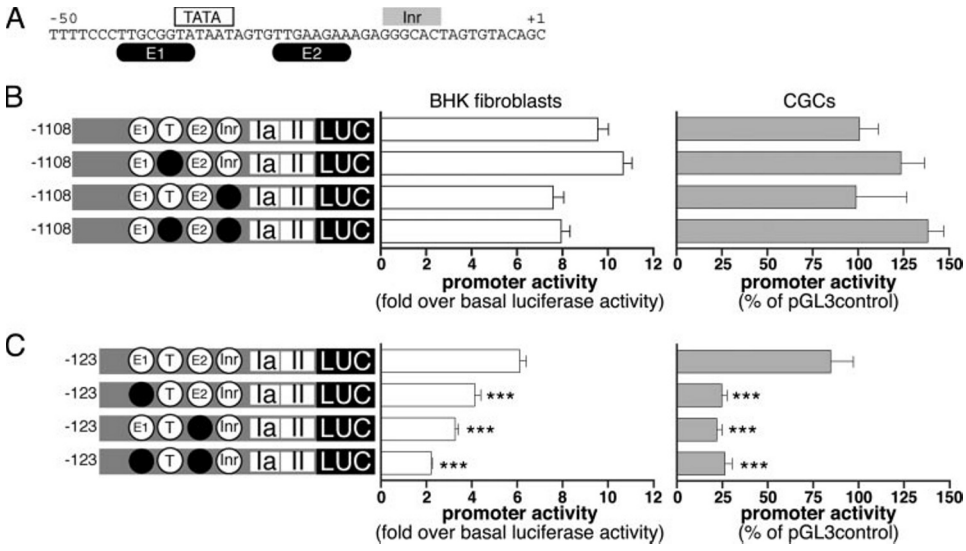

FIGURE 4. **Luciferase assays on the exon Ia promoter region with targeted mutations of predicted transcription factor binding elements.** *A*, schematic representation of mGlu1 core promoter sequence with mutated putative elements highlighted. *B* and *C*, schematic diagrams of reporter gene constructs used in luciferase assays. For BHK cells, activity is given as -fold over pGL3-basic (*white bars*). For CGCs activity is indicated as percentage of pGL3-control (*gray bars*). *B*, effect of the mutation of the putative TATA box and Inr element upstream from exon Ia. Data are representative of at least 18 and four replicates for BHK cells and CGCs, respectively. Statistical significance is relative to construct −1108/ExIa. *C*, effect of the mutation of E1 and E2 elements. Data are representative of at least eight and six replicates for BHK cells and CGCs, respectively. Statistical significance is relative to construct −123/ExIa. *, $p < 0.05$; **, $p < 0.01$; ***, $p < 0.001$, ANOVA with Bonferroni's *post hoc* test.

TABLE 3
Sequence of the elements mutated in reporter gene experiments

Construct	Wild type sequence	Mutated sequence	Template
−1108/ExIa/TATAm (35)	CCCTTGCGGTATAATAGTGT	CCCTTGCGGTggAATAGTGT	−1108/ExIa
−1108/ExIa/INIm (36)	AAAGAGGGCACTAGTGTACA	AAAGAGGGggCTAGTGTACA	−1108/ExIa
−123/ExIa/E1m	TTTCCCTTGCGGTATAATAG	TTTCCC-gaattc-TAATAG	−123/ExIa
−123/ExIa/E2m	ATAGTGTTGAAGAAAGAGGG	ATAGTG-gaattc-AGAGGG	−123/ExIa
−1108/*Grm1*/NRSEm (38)	GAGCGCTGTCCAGGGTTCTG	GAGCGCTGTaaAGGGTTCTG	−1108/*Grm1*
+478/+899/*Grm1*/NRSEm	GAGCGCTGTCCAGGGTTCTG	GAGCGCTGTaaAGGGTTCTG	+478/+899/SV40
+895/ExII/RFXm	GGCGTTGCCTTAGTAACTAA	GGCG----aatt----CTAA	+895/ExII

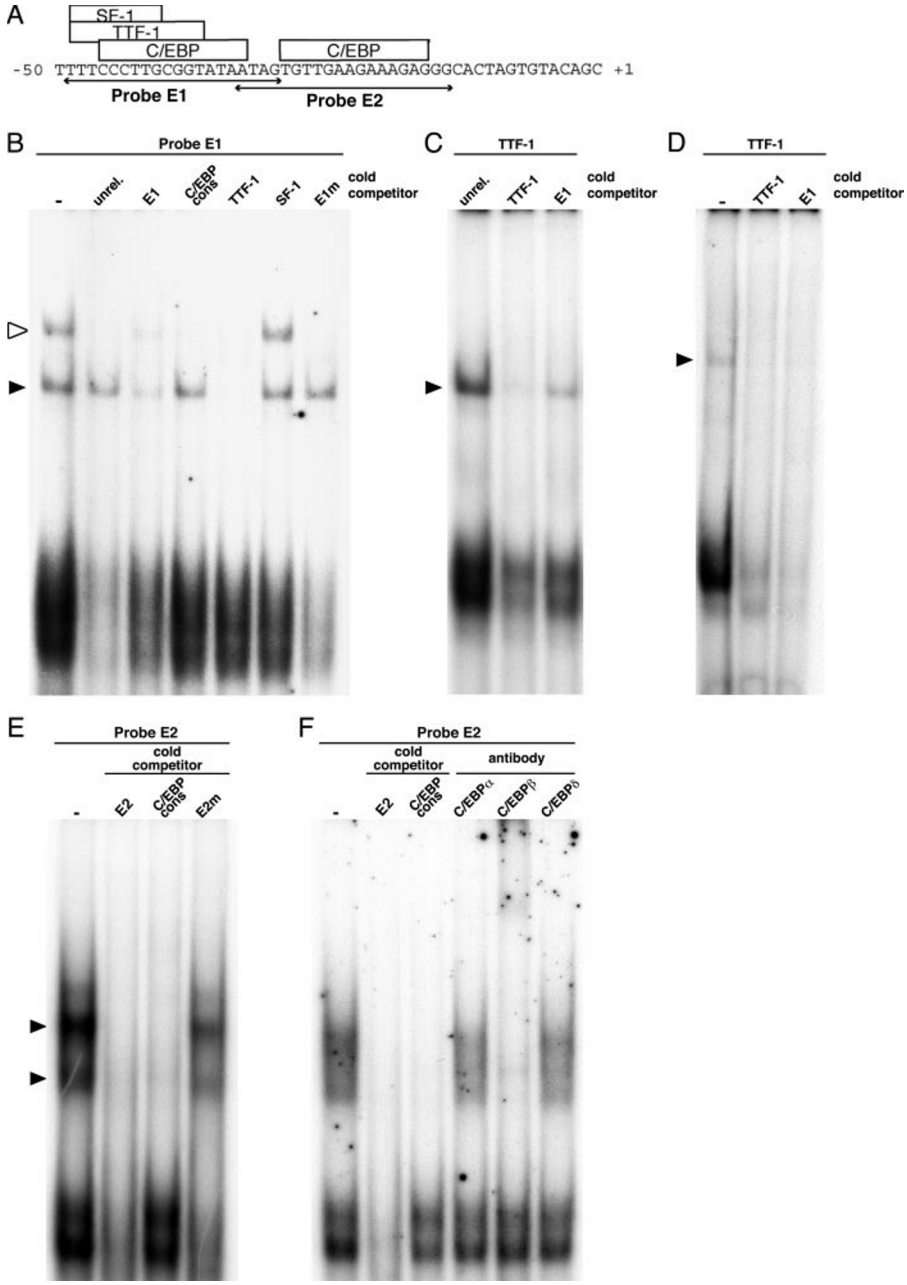

FIGURE 5. **EMSA on exon Ia core promoter region.** *A*, sequence of exon Ia core promoter region. Transcription factor binding sites and extent of oligonucleotides are indicated. *B*, EMSA analysis of transcription factors binding to probe E1. Radiolabeled probe E1 incubated with nuclear extracts from mouse cerebellum produced a specific band (*filled arrowhead*) competed by a consensus probe for TTF-1 and a nonspecific band (*open arrowhead*) competed by several probes. The TTF-1 consensus probe, incubated with nuclear extracts from mouse cerebellum (*C*) or from CGCs (*D*), produced a band (*filled arrowhead*) that is almost completely competed by unlabeled probe E1. *E*, EMSA analysis of transcription factors binding to probe E2. Radiolabeled probe E2 incubated with nuclear extracts from BHK cells produced at least two bands (*filled arrowheads*), which were competed by the C/EBP consensus probe. *F*, supershift analysis of C/EBP factors binding to probe E2. Anti-C/EBPβ, but not anti-C/EBPα and -∂ antibodies, produced a supershift of the two bands generated by probe E2.

most significantly, from mouse liver or cerebellum (Fig. 6*C*). We chose the NIH-3T3 cell line, and not BHK cells, because it derives from mice; hence, all of the genomic sequences required for these experiments were known.

The repressive action on transcription of NRSF is mediated by the recruitment, among others, of co-repressors having histone deacetylase (HDAC) activity. We assessed whether the repression of *Grm1* transcription is HDAC-dependent by treating NIH-3T3 fibroblasts with the HDAC inhibitor TSA and then by analyzing mGlu1 expression by RT-PCR (Fig. 6*D*). Specific oligonucleotides located on exons VIII and X were designed in order to detect the mGlu1α and -β splice variants. Mouse cerebellum cDNA was used as positive control, from which two fragments of 524 and 609 bp were amplified, corresponding to mGlu1α and -β isoforms, respectively. Weak but detectable levels of mGlu1 transcripts were present in nonstimulated NIH-3T3 cells, whereas TSA significantly induced the expression of mGlu1β and slightly induced the expression of mGlu1α (Fig. 6*D*). The effect of TSA upon NRSF action on *Grm1* transcription was also verified in luciferase assays on BHK cells and performed using the plasmid +478/+899/SV40 carrying either the intact or the mutated NRSE. A 24-h treatment with 300 nM TSA reduced the luciferase activity of the pGL3-promoter vector to 83.3 ± 2.9% (n = 10). Conversely, in cells transfected with construct +478/+899/SV40, TSA partially reverted the inhibitory effect of the NRSE on the SV40 promoter increasing the luciferase activity of this constructs from 21.5 ± 9.5% to 32.0 ± 8.4% ($p < 0.05$; ANOVA with Bonferroni's *post hoc* test; $n = 12$) relative to the untreated pGL3-promoter. In other words, the repressive action of NRSF was blocked by TSA treatment, thus enhancing the transcriptional activity of +478/+899/SV40 construct. When the NRSE was mutated, TSA produced a nonsignificant reduction of the luciferase activity induced by +478/+899/SV40/NRSEm from 58.8 ± 2.6 to 52.5 ± 1.6% ($p = 0.06$; $n = 12$), similar to what was observed with the pGL3-promoter. Therefore, histone deacetylation appears as a key mechanism by which NRSF regulates mGlu1 expression in nonneuronal cells.

Identification of an Active RFX Element Regulating Grm1 Expression in Nonneuronal Cells—The finding that the region +895/+1088 upstream from exon II may contain a silencing element active in fibroblasts prompted us to investigate the role of the putative RFX element located at positions +951/+968. We performed a new series of luciferase assays on BHK cells,

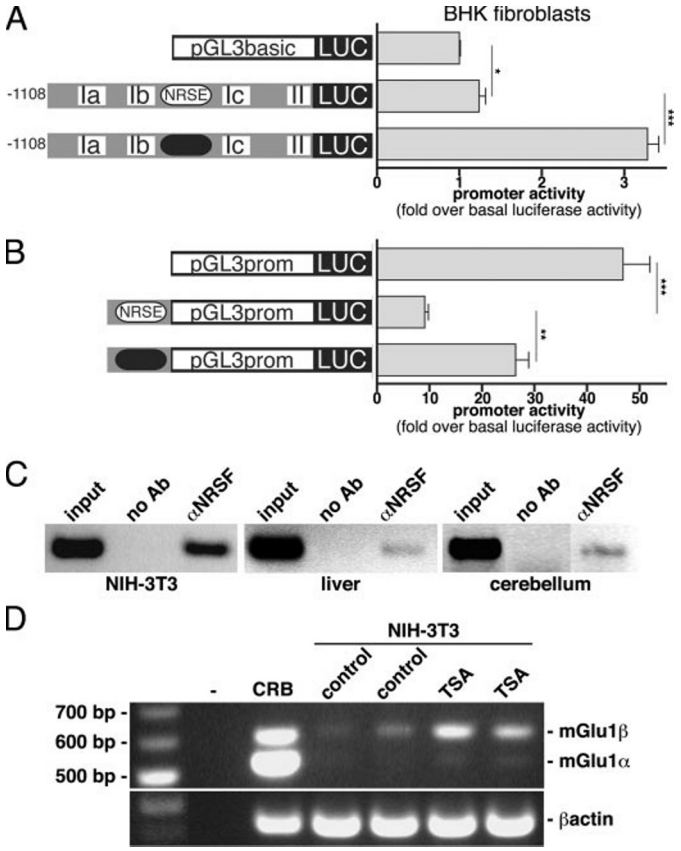

FIGURE 6. **Characterization of NRSF action on *Grm1* expression.** *A* and *B*, schematic diagrams of reporter gene constructs and corresponding activity in BHK cells, indicated as -fold over pGL3-basic. *A*, luciferase activity of a 3-kbp region at the 5′-end of *Grm1* and effect of mutation of NRSE. Data are representative of at least 18 replicates. Statistical significance is relative to construct −1108/*Grm1*. *B*, effect of wild type and mutated NRSE from *Grm1* on SV40 promoter. Data are representative of at least 18 replicates. Statistical significance is relative to construct +478/+899/SV40. ANOVA with Bonferroni's *post hoc* test (*, $p < 0.05$; **, $p < 0.01$; ***, $p < 0.001$). *C*, ChIP assays showing *in vivo* binding of NRSF to *Grm1* promoter region, performed on NIH-3T3 cells, mouse liver, and cerebellum. *D*, RT-PCR analysis of mGlu1α, mGlu1β, and β-actin expression in NIH-3T3 cells. Cells were stimulated for 24 h with 200 nM TSA and cultured for an additional 24 h.

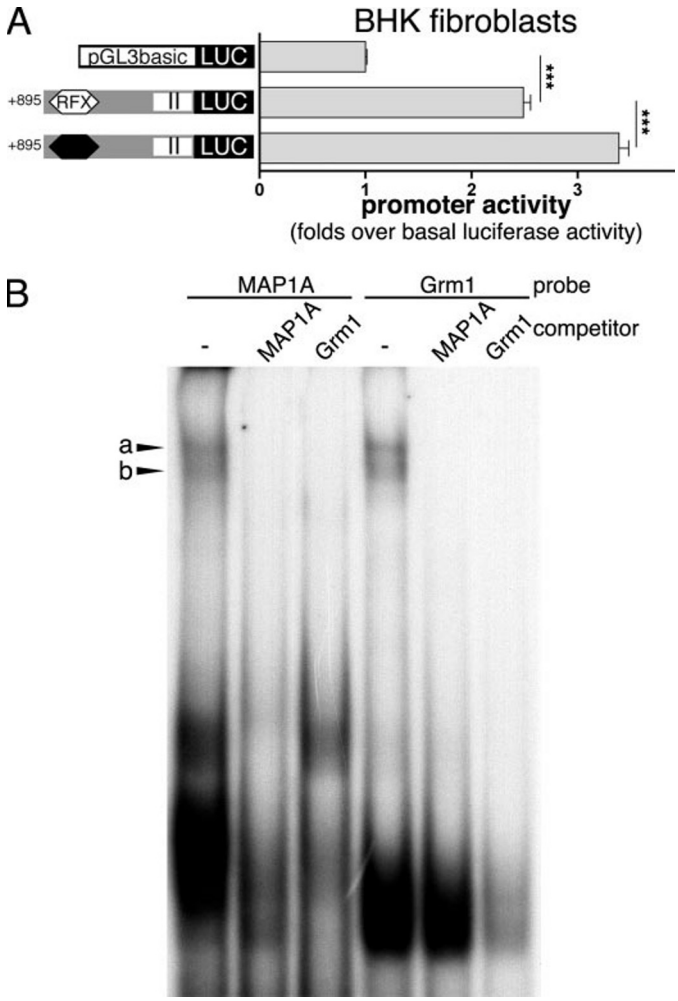

FIGURE 7. **Functional characterization of the RFX element.** *A*, analysis of the effect of *Grm1* RFX element on exon II promoter activity. Shown are schematic diagrams of reporter gene constructs and corresponding activity in BHK cells, indicated as -fold over pGL3-basic. Data are representative of at least eight replicates. *B*, EMSA analysis of RFX factor DNA binding activity in nuclear extracts from BHK cells incubated with radiolabeled probes encoding the *MAP1A*-RFX element or the *Grm1*-RFX element. Both probes produce two shifted bands that are competed by RFX-*MAP1A* and RFX-*Grm1* unlabeled probes. *, $p < 0.05$; **, $p < 0.01$; ***, $p < 0.001$, ANOVA with Bonferroni's *post hoc* test.

analyzing the transcriptional activity of plasmid +895/ExII carrying a mutation in the RFX element (see Table 3). The mutation of the RFX element enhanced the transcriptional activity of plasmid +895/ExII from 2.4 ± 0.2- to 3.4 ± 0.4-fold over pGL3-basic, an increase that was in the same range of that resulting from the deletion of the region +895/+1088 (Fig. 7*A*). Subsequently, we verified the actual binding of a factor of the RFX family by EMSA in nuclear extracts from BHK fibroblasts (Fig. 7*B*). A probe deriving from the promoter of the *MAP1A* gene (30) was used to assess the presence of active RFX factors both in BHK nuclear extracts and in competition experiments. Incubation of radiolabeled RFX-*MAP1A* probe with BHK nuclear extracts produced at least four shifted bands. The upper two bands (Fig. 7*B*) were clearly displaced by the unlabeled RFX-*Grm1* probe, encoding the sequence of the RFX element present upstream from exon II. Consistently, the radiolabeled RFX-*Grm1* probe produced three bands, two of which corresponded in terms of apparent molecular weight to the high ones obtained with the RFX-*MAP1A* probe (Fig. 7*B*). Competition experiments then showed that an excess of unlabeled RFX-*MAP1A* probe was able to displace these bands (Fig. 7*B*).

Taken together, these data indicate that the RFX element, located upstream from exon II, has a role in down-regulating transcriptional activity of *Grm1* in nonneuronal cells.

DISCUSSION

In this study, we have performed the first detailed analysis of the *Grm1* structure and identified the transcription factors and *cis*-acting elements involved in its transcriptional regulation and neuron-specific expression. We show by different experimental means that transcription at both murine and human *Grm1* initiates, through multiple promoters, from alternative first exons. This feature is shared by mGlu5 (6), the other phospholipase C-coupled mGlus, and appears frequent in mammalian genes (39). 5′-RACE and RT-PCR experiments revealed the relative abundance of mRNA containing exons Ia–Ic and II in

the mouse brain. We estimated that ~70% of mGlu1 transcripts start within exon Ia and that the remaining start within exon II, since transcripts containing exon Ib or Ic were rarely found and exhibited a pattern of expression mostly restricted to the cerebellum.

Comparison between the human, rat, and mouse *Grm1* showed a very similar structural organization and a high degree of sequence identity at both translated and untranslated regions. Phylogenetic shadowing analysis performed on 5.2 kb at the 5′-end of *Grm1* of seven different mammalian species highlighted several evolutionarily conserved regions upstream from alternative first exons as well as two *cis*-elements corresponding to a NRSE and RFX.

One of the primary findings of this study is the characterization of a promoter module constituted of a TTF-1 and a C/EBP element necessary for the recruitment of the basal transcriptional complex and transcription of mGlu1 mRNAs containing exon Ia. The binding of TTF-1 and C/EBP to the murine *Grm1* exon Ia promoter and the synergistic interaction between these two factors was demonstrated in neural tissue by EMSA and reporter gene assays using cerebellar nuclear extracts and primary cultures of cerebellar neurons, respectively.

TTF-1 is a member of the homeodomain NK family of transcription factors and has a prominent role in cell-specific gene regulation in thyroid and lung (40). Despite the fact that expression of TTF-1 in the central nervous system has also been reported, in particular in neurons enriched in mGlu1 (9), such as Purkinje cells, principal neurons of the hippocampus, and the retina (41), this is the first report of a neuronal target gene of TTF-1. However, transcriptional regulation of the α7 nicotinic acetylcholine receptor by TTF-1, although in Clara cells of the lung, has recently been reported (42).

C/EBP proteins form a family of basic leucine zipper transcription factors composed of five members (43). Within the rodent central nervous system, C/EBPβ expression appears compatible with its role in the regulation of mGlu1 transcription. Transcripts encoding C/EBPβ were detected in Purkinje and granule cells of the cerebellum as well as in principal cells and interneurons of the hippocampal formation (44). Interestingly, PC12 cells were shown to respond to NGF stimulation by enhancing the expression of both C/EBPβ (44) and mGlu1 (45).

A cooperative action between C/EBPα and TTF-1 has been proposed for the promoter of the *CCSP/UG* gene in lung Clara cells (46). For the induction of transcription at the *CCSP/UG* promoter, each of these factors appeared necessary but not sufficient (46), similar to what we observed for the *Grm1* promoter. Therefore, we propose that proximal TTF-1-C/EBP elements represent a transcriptional module in which the interplay of (at least) two transcription factors activates transcription synergistically (47). This module is radically different from the known core promoter modules, such as TATA-Inr or Inr-DPE (27), which are generally present in genes characterized by a widespread expression or by an expression profile restricted to a unique but homogeneous tissue. It is thus conceivable that genes with a complex and highly restricted expression pattern, such as *Grm1*, possess core promoters with almost unique features.

Additional factors are likely to participate in the cell- and context-specific transcriptional regulation of mGlu1. Indeed, our deletion scan analysis showed that modification of region ΔD, which does not overlap with the TTF-1 and C/EBP elements, also markedly influenced transcriptional activity, suggesting the presence of a further element(s). However, our *in silico* analysis could not identify any putative transcription factor binding site within this region, possibly because of its low level of conservation across species.

A surprising finding was the lack of effects, under our experimental conditions, of the specific mutations of the TATA box and Inr elements because of their well known role in core promoters in many eukaryotic genes (27). The prediction of false positive transcription factor binding sites is a critical issue for most sequence analysis tools (25); hence, the functional validation of any predicted element remains imperative. However, we cannot at present rule out that this module may be active, as an alternative core promoter, in a different cell model or context.

Functional analysis of the promoter region upstream from exon II showed a weak but significant luciferase activity in both BHK cells and CGCs that was enhanced by the 5′-deletion of 193 bp. As we demonstrated by site-specific mutation and EMSA experiments, this effect was due to the presence in this region of a repressor, namely an RFX element. Four members of the murine RFX family have been identified so far (30), but their role as regulators of transcriptional events is still largely unclear. For instance, the promoter of the *MAP1A* gene was repressed by RFX1 and -3 in nonneuronal cells (30), whereas expression of the glutamate transporter EAAT3 was enhanced by RFX1 (31). Our data provide further evidence supporting a role for RFX factors as transcriptional repressors for the specification of the expression of neuronal genes.

A recent genome-wide analysis has identified 1894 genes in the mouse genome (1892 in the human genome) as putative targets of NRSF (29). However, for only ~30 genes has substantial experimental evidence for the silencing action of NRSF been provided so far, and for even fewer genes has the actual interaction of NRSF with its endogenous target gene *in vivo* been examined (29). Here, we have shown that *Grm1* possesses an NRSE, which was able to specifically repress transcription in nonneuronal cells, namely fibroblasts. Moreover, we demonstrated the actual binding of NRSF to this element *in vivo* by means of chromatin immunoprecipitation. Therefore, our data clearly identify NRSF as a master switch allowing mGlu1-specific expression in neuronal cells while keeping it silenced in nonneuronal tissues. A few studies have reported expression of mGlu1 in nonneuronal tissues, such as osteoblasts (48) and cardiomyocytes (49). These findings suggest that under certain conditions, silencing by NRSF may be inactive on the transcriptional activity of the *Grm1* promoter(s). It is worth noting that also for the NMDA receptor subunit 2C, whose promoter region contains a NRSE consensus element too (2), expression has been detected in osteoblasts (48). Our data further provide some insights about the mechanism of action of NRSF on *Grm1* transcription, since we showed that the silencing action is mediated by histone deacetylases. We indeed demonstrated that the HDAC inhibitor TSA was able to up-regulate mGlu1α and -β expression in NIH-3T3 cells and to inhibit the repress-

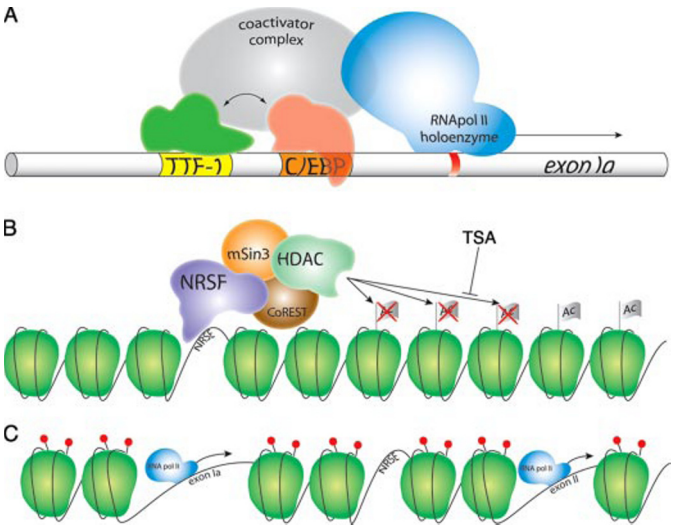

FIGURE 8. **Proposed model describing the transcriptional activation of *Grm1*.** *A*, the core promoter region upstream from exon Ia is synergistically activated by TTF-1 and C/EBPβ transcription factors, which recruit the RNA polymerase II transcriptional complex. *B*, in differentiated nonneuronal cells, NRSF recruits a macromolecular complex that induces chromatin packing and prevents *Grm1* transcriptional activation. Histone deacetylation appears to be involved. *C*, in neurons, chromatin structure is permissive, as indicated also by H3K4 di- and trimethylation (*red circles*). Hence, transcription factors can access *Grm1* promoters.

ing activity of NRSE on the SV40 promoter. It was surprising to find detectable levels of mGlu1 expression in NIH-3T3 cells, despite the silencing role of NRSF. However, since NIH-3T3 cells are an immortalized cell line, it is possible that the state of their chromatin is poised for expression of neuronal genes with NRSF promoting only the deacetylation of histones, thus allowing low levels of transcription, as also observed in stem cells (50). Conversely, in terminally differentiated nonneuronal cells, NRSF drives efficient chromatin packing and DNA methylation. Therefore, in NIH-3T3 cells, transcription at *Grm1* might occur at very low rates, and TSA treatment appeared sufficient to enhance it.

Dysregulated expression of mGlu1 was shown to produce very important pathological consequences, since melanoma onset was found to result from aberrant mGlu1 expression in both mouse and human melanocytes (20). Our findings may provide the molecular background to understand the mechanism(s) responsible for the defective regulation of mGlu1 expression in these cells. For instance, in neoplastic melanocytes, a mutation/deletion of the NRSE located within *Grm1* could prevent the binding of NRSF and in turn allow mGlu1 expression.

In conclusion, constitutive transcription at the core promoter upstream from exon Ia, which is most likely the main mGlu1 promoter, is driven by the synergistic interaction of TTF-1 and C/EBPβ. These factors may then recruit a multimeric complex composed of co-activators and the RNA polymerase II holoenzyme, resulting in the transcription of mGlu1. Beyond core promoter activation, a second level of regulation may be provided in nonneuronal cells by NRSF that, either through CoREST or mSin3, recruits HDACs, which in turn induce chromatin packing and transcriptional repression. In neurons, the NRSF action is inhibited, and the chromatin at *Grm1* assumes an open conformation (*e.g.* H3K4 is di- and trimethylated) (51); thus, transcription factors would have access to the exon Ia promoter, inducing mGlu1 expression. A schematic diagram for the transcriptional control of *Grm1* is given in Fig. 8.

Therefore, our data indicate that the cell-specific expression of mGlu1 is determined by the combined activity of discrete repressing elements, such as NRSE and RFX, as well as by positive regulatory elements that are active in specific types of neuron.

Acknowledgments—We thank C. Berlato, W. Doppler (Department of Medical Biochemistry, Innsbruck Medical University), and C. Sala (DIBIT, Milano, Italy) for helpful suggestions. We also gratefully acknowledge Sabine Schönherr (Dept. Pharmacology, Innsbruck Medical University) for excellent technical support.

REFERENCES

1. Nakanishi, S. (1992) *Science* **258,** 597–603
2. Myers, S. J., Dingledine, R., and Borges, K. (1999) *Annu. Rev. Pharmacol. Toxicol.* **39,** 221–241
3. Borges, K., and Dingledine, R. (2001) *J. Biol. Chem.* **276,** 25929–25938
4. Chew, L., Yuan, X., Scherer, S., Qie, L., Huang, F., Hayes, W., and Gallo, V. (2001) *J. Biol. Chem.* **276,** 42162–42171
5. Corti, C., Xuereb, J. H., Corsi, M., and Ferraguti, F. (2001) *Biochem. Biophys. Res. Commun.* **286,** 381–387
6. Corti, C., Clarkson, R. W., Crepaldi, L., Sala, C. F., Xuereb, J. H., and Ferraguti, F. (2003) *J. Biol. Chem.* **278,** 33105–33119
7. Liu, A., Zhuang, Z., Hoffman, P., and Bai, G. (2003) *J. Biol. Chem.* **278,** 26423–26434
8. Conn, P., and Pin, J. (1997) *Annu. Rev. Pharmacol. Toxicol.* **37,** 205–237
9. Ferraguti, F., and Shigemoto, R. (2006) *Cell Tissue Res.* **326,** 483–504
10. Tanabe, Y., Masu, M., Ishii, T., Shigemoto, R., and Nakanishi, S. (1992) *Neuron* **8,** 169–179
11. Laurie, D. J., Boddeke, H. W., Hiltscher, R., and Sommer, B. (1996) *Eur. J. Pharmacol.* **296,** R1–R3
12. Zhu, H., Ryan, K., and Chen, S. (1999) *Brain Res. Mol. Brain Res.* **73,** 93–103
13. Berthele, A., Laurie, D. J., Platzer, S., Zieglgansberger, W., Tolle, T. R., and Sommer, B. (1998) *Neuroscience* **85,** 733–749
14. Ferraguti, F., Conquet, F., Corti, C., Grandes, P., Kuhn, R., and Knopfel, T. (1998) *J. Comp. Neurol.* **400,** 391–407
15. Ferraguti, F., Cobden, P., Pollard, M., Cope, D., Shigemoto, R., Watanabe, M., and Somogyi, P. (2004) *Hippocampus* **14,** 193–215
16. Shigemoto, R., Nakanishi, S., and Mizuno, N. (1992) *J. Comp. Neurol.* **322,** 121–135
17. Lopez-Bendito, G., Shigemoto, R., Fairen, A., and Lujan, R. (2002) *Cereb. Cortex* **12,** 625–638
18. Conquet, F., Bashir, Z., Davies, C., Daniel, H., Ferraguti, F., Bordi, F., Franz-Bacon, K., Reggiani, A., Matarese, V., Conde, F., Collingridge, G. L., and Crepel, F. (1994) *Nature* **372,** 237–243
19. Kano, M., Hashimoto, K., Kurihara, H., Watanabe, M., Inoue, Y., Aiba, A., and Tonegawa, S. (1997) *Neuron* **18,** 71–79
20. Marin, Y. E., and Chen, S. (2004) *J. Mol. Med* **82,** 735–749
21. Kuramoto, T., Maihara, T., Masu, M., Nakanishi, S., and Serikawa, T. (1994) *Genomics* **19,** 358–361
22. Stephan, D., Bon, C., Holzwarth, J. A., Galvan, M., and Pruss, R. M. (1996) *Neuropharmacology* **35,** 1649–1660
23. Trenckner, E. (1991) *Culturing Nerve Cells: Cerebellar Cells in Culture*, MIT Press, Cambridge, MA
24. Schwartz, S., Elnitski, L., Li, M., Weirauch, M., Riemer, C., Smit, A., Green, E., Hardison, R., and Miller, W. (2003) *Nucleic Acids Res.* **31,** 3518–3524
25. Ovcharenko, I., Loots, G. G., Giardine, B. M., Hou, M., Ma, J., Hardison, R. C., Stubbs, L., and Miller, W. (2005) *Genome Res.* **15,** 184–194
26. Loots, G. G., and Ovcharenko, I. (2004) *Nucleic Acids Res.* **32,** W217–W221

27. Smale, S. T., and Kadonaga, J. T. (2003) *Annu. Rev. Biochem.* **72,** 449–479
28. Storring, J., Charest, A., Cheng, P., and Albert, P. (1999) *J. Neurochem.* **72,** 2238–2247
29. Bruce, A. W., Donaldson, I. J., Wood, I. C., Yerbury, S. A., Sadowski, M. I., Chapman, M., Gottgens, B., and Buckley, N. J. (2004) *Proc. Natl. Acad. Sci. U. S. A.* **101,** 10458–10463
30. Nakayama, A., Murakami, H., Maeyama, N., Yamashiro, N., Sakakibara, A., Mori, N., and Takahashi, M. (2003) *J. Biol. Chem.* **278,** 233–240
31. Ma, K., Zheng, S., and Zuo, Z. (2006) *J. Biol. Chem.* **281,** 21250–21255
32. Rich, A., and Zhang, S. (2003) *Nat. Rev. Genet.* **4,** 566–572
33. Aronica, E., Dell'Albani, P., Condorelli, D., Nicoletti, F., Hack, N., and Balazs, R. (1993) *Mol. Pharmacol.* **44,** 981–989
34. Bessho, Y., Nawa, H., and Nakanishi, S. (1993) *J. Neurochem.* **60,** 253–259
35. Wang, K., Krause, P. R., and Straus, S. E. (1995) *J. Virol.* **69,** 2873–2880
36. Lo, K., and Smale, S. T. (1996) *Gene* (*Amst.*) **182,** 13–22
37. Lee, B., Cho, G., Norgren, R. J., Junier, M., Hill, D., Tapia, V., Costa, M., and Ojeda, S. (2001) *Mol. Cell Neurosci.* **17,** 107–126
38. Toshiyuki, N., and Ichiro, M. (2004) *Brain Res. Mol. Brain Res.* **125,** 47–59
39. Landry, J. R., Mager, D. L., and Wilhelm, B. T. (2003) *Trends Genet.* **19,** 640–648
40. Bingle, C. (1997) *Int. J. Biochem. Cell Biol.* **29,** 1471–1473
41. Suzuki, K., Kobayashi, Y., Katoh, R., Kohn, L., and Kawaoi, A. (1998) *Endocrinology* **139,** 3014–3017
42. Reynolds, P., and Hoidal, J. (2005) *J. Biol. Chem.* **280,** 32548–32554
43. Lekstrom-Himes, J., and Xanthopoulos, K. G. (1998) *J. Biol. Chem.* **273,** 28545–28548
44. Sterneck, E., and Johnson, P. F. (1998) *J. Neurochem.* **70,** 2424–2433
45. Kane, M. D., Vanden Heuvel, J. P., Isom, G. E., and Schwarz, R. D. (1998) *Neurosci. Lett.* **252,** 1–4
46. Nord, M., Cassel, T., Braun, H., and Suske, G. (2000) *Ann. N. Y. Acad. Sci.* **923,** 154–165
47. Werner, T., Fessele, S., Maier, H., and Nelson, P. J. (2003) *FASEB J.* **17,** 1228–1237
48. Gu, Y., and Publicover, S. J. (2000) *J. Biol. Chem.* **275,** 34252–34259
49. Gill, S. S., Pulido, O. M., Mueller, R. W., and McGuire, P. F. (1999) *Brain Res. Bull.* **48,** 143–146
50. Ballas, N., Grunseich, C., Lu, D. D., Speh, J. C., and Mandel, G. (2005) *Cell* **121,** 645–657
51. Stadler, F., Kolb, G., Rubusch, L., Baker, S., Jones, E., and Akbarian, S. (2005) *J. Neurochem.* **94,** 324–336